

2021.12.02 Interferometry Experiment

Start Time: circa 09.00

Aim

An experiment was carried out to ascertain the thickness of a soap film on the nanometre scale, using interferometric techniques, in order to acquaint ourselves with the level of precision of these tools, as well as to gain experience using research-level optics equipment. By comparing the interference pattern of the split beams before and after placing a film, we are able to arrive at a value for the thickness of the film, given that $n = 1.33$.

Background

There are several geometric constructions used for interferometers (such as the LIGO detectors used to observe gravitational waves), but the Mach-Zehnder configuration was found to be the most suitable, as shown in the figure below:

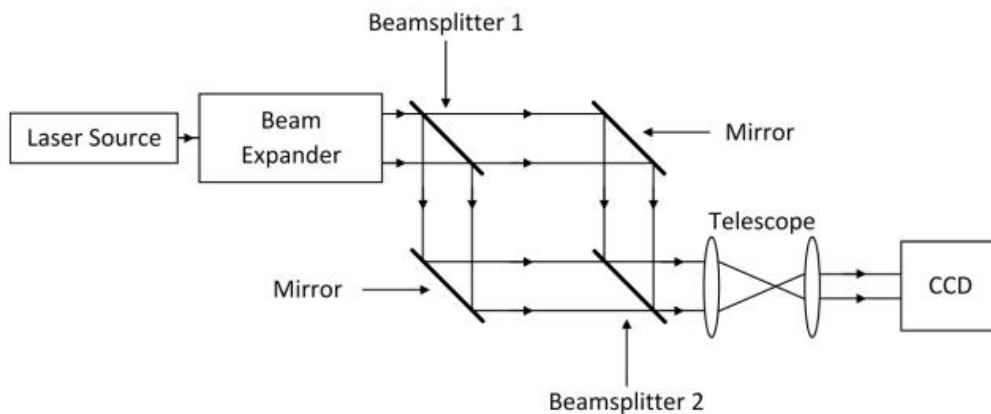


Figure 0: simplified schematic of a Mach-Zehnder setup

Source: Mangles et. al, 2021, "Year 1 Laboratory Manual: Interferometer Experiment", Imperial College

As shown above, the laser source is fed into a beam expander, which utilises a lens to increase the diameter of the beam: therefore, upon hitting beamsplitter 1, half of the light is transmitted to one mirror at an angle along the original beam axis, whereas another half is reflected towards a second mirror, at an the incident angle. These two split beams are reflected off two distinct mirrors, before reconverging again at beamsplitter 2, where they pass through a reducing telescope to decrease the beam diameter back down to a size similar to the camera's CCD chip. This camera then captures an image, or a series of images at 100FPS (in the form of a TIF video file) of the object, outputting a fringe pattern which will be used in the analysis of the phase shift caused by one of these beams passing through a medium with a different refractive index to air.

Fringe shift occurs upon the placement of an object (i.e. the soap film) with a refractive index different to that of air, in the path of one of the split beams between the beamsplitters 1 and 2. This introduces a phase difference upon the two beams' arrival at the CCD, which will shift the fringe pattern perpendicular to their length. An example of this is shown below with a lit and unlit candle.

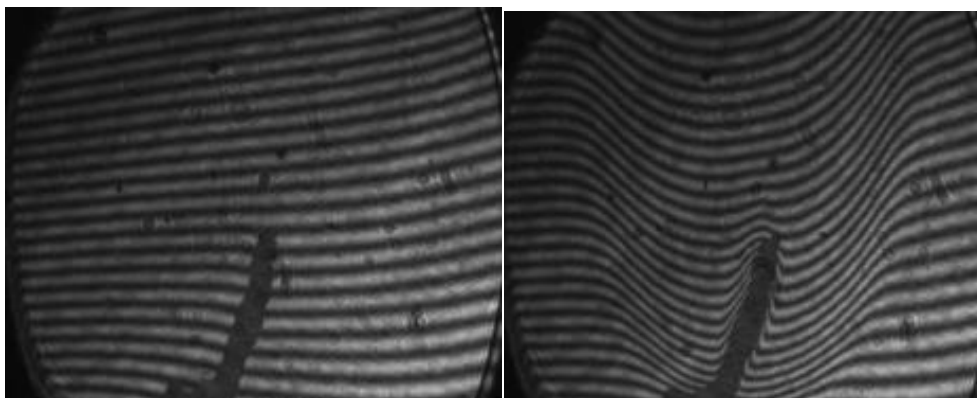


Figure 1: the fringe shift due to a candle flame's presence in the object beam.
(Left) - shows the unlit candle, (Right) - shows the lit candle

Source: Mangles et. al, 2021, "Year 1 Laboratory Manual: Interferometer Experiment", Imperial College

By taking the refractive index of air to be 1 (i.e. $N_{\text{air}} = 1$), we have that phase shift $\Delta\Phi$ (in radians) introduced through the insertion of an object thickness x (m) with N_{object} in the path of one of the beams is given by:

$$\Delta\Phi = \Phi_{\text{object}} - \Phi_{\text{air}} = \frac{2 \cdot \pi \cdot x \cdot N_{\text{object}}}{\lambda} - \frac{2 \cdot \pi \cdot x \cdot N_{\text{air}}}{\lambda} = \frac{2 \cdot \pi \cdot x}{\lambda} (N_{\text{object}} - N_{\text{air}}) \approx \frac{2\pi x}{\lambda} (N_{\text{object}} - 1) \quad (1)$$

Thus, from using the fringe shift, F , which gives the number of fringes a given fringe has moved by upon the introduction of another object, we can determine $\Delta\Phi$ which gives the phase shift. Consequently, we can determine that $\Delta\Phi \approx 2\pi F$, i.e. for $F=1$, this corresponds to $\Delta\Phi = 2\pi$. By equating these two expressions for $\Delta\Phi$, we can find x , N_{object} , λ and F are related by the following expression when measured from the CCD image:

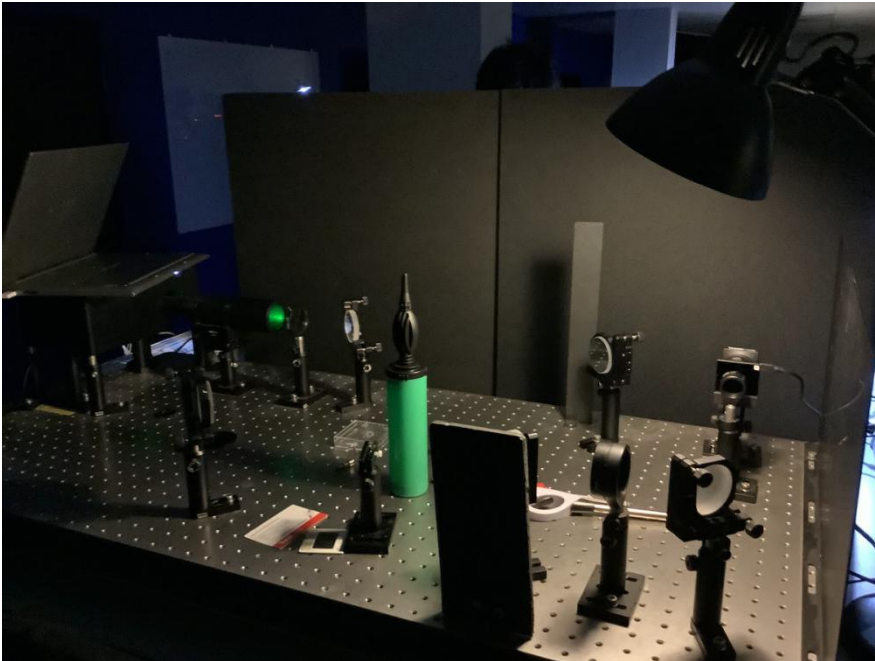
$$\lambda \cdot F \approx x(N_{\text{object}} - 1) \quad (2)$$

Description of Set Up

Safety:

Due to the dangerous nature of lasers, care was taken to ensure that it was turned off when it was not in use, and that the default set-up was left unaltered, besides the screws, to prevent unnecessary accidents. Reflective objects and reflexions were made sure to be eliminated for the duration of the experiment.

The Mach-Zehnder interferometer for the following experiment had already been set-up by the lab technicians, and consisted of a pinhole system (optical breadboard) that can be described by the following images shown below:





The set-up consisted of the following: a laser source, contained with the safety enclosure; the first beamsplitter; the probe beam, which is the beam reflected by beamsplitter 1 which passes through the objects of different refractive indexes to that of air; the probe mirror, which reflects the probe beam towards beamsplitter 2; the reference beam, which continues to be transmitted through beamsplitter 1; the reference mirror, the mirror that reflects the reference beam towards beamsplitter 2.

Measurement Strategy

In order to align the interferometer, the following steps were carried out:

(1) turn on laser. (2) close the iris, after the beam expander to only allow a trickle of light, which marks the centrepont of the beam. (3) adjust the reference mirror, whilst blocking the probe beam with a piece of card, centering the beam onto beamsplitter 2. (4) the repeat the above step for the probe mirror.

In order to adjust the CCD camera, the following was done:

(1) turn on ThorCam on Windows laptop which camera is connected to. (2) enter Live View. (3) by examining the histogram, reduce exposure time such that not too many of the pixels are reading at the maximum intensity, in which case the image is overexposed, and the camera is saturated.

In order to focus the camera:

(1) block out reference beam. (2) place a filter with letters and shapes (e.g. three bar chart slide). (3) loosen the bolts of the filter holder on the breadboard. (4) adjust position of filter holder forwards and backwards until you have a crisp image - objects in this position will be imaged onto the CCD. (5) bolt down the filter holder again to the breadboard once satisfied that the lens is focused.

Once the image has been focused, we can now produce interference fringes and make interferometric measurements from these: (1) white card was placed at the focal point between the two telescope lenses, and motion control was used on beamsplitter 2 to ensure the two beam positions at the focal points between the telescope lenses overlap (which can be seen as a bright dot on the card paper) overlap to produce parallel beams upon exiting the second lens. (2) align the beams to the centre of the smaller, second lens placed before the camera.

Now to measure the soap bubbles, the following was carried out:

(1) soap bubble was placed in the path of the beam, a video was recorded of the bubble popping, with the recording ending when the bubble pops. A more coherent image was obtained at the boundaries of the fringe shift when the bubble stopped rippling. (2) pictures of fringes right before and after the bubble pops taken.

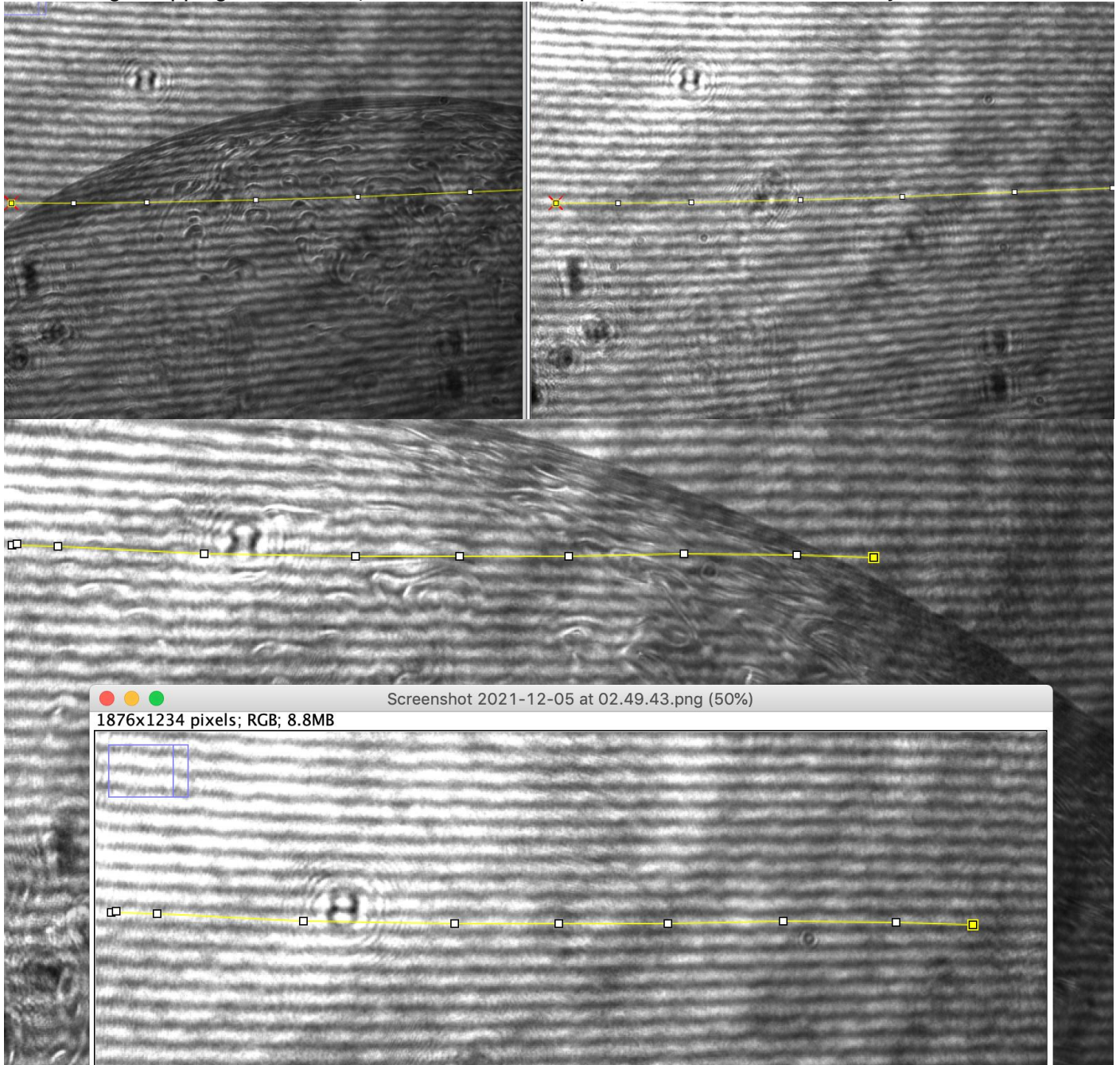
In order to determine the fringe shift, on ImageJ, the Synchronise Windows tool was used to display both images side-by-side. Then, a constructive or destructive interference fringe appears just outside the bubble, so a segmented line tool was used. On the image without the bubble, points are clicked along the same curve

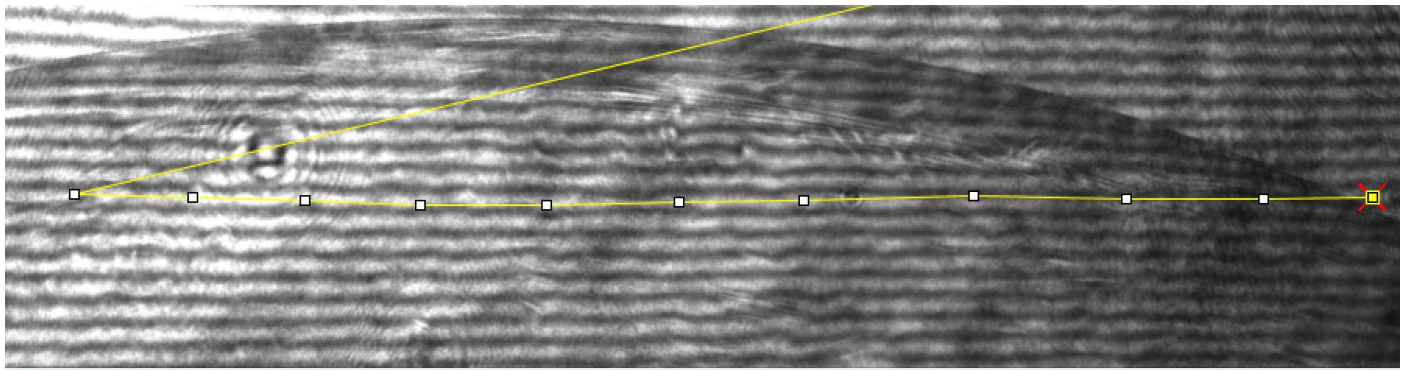
as the fringe shown whilst using the segmented line tool, and the number of fringes that the line intersects on the image with the bubble is chosen to be our F value.

Raw Data

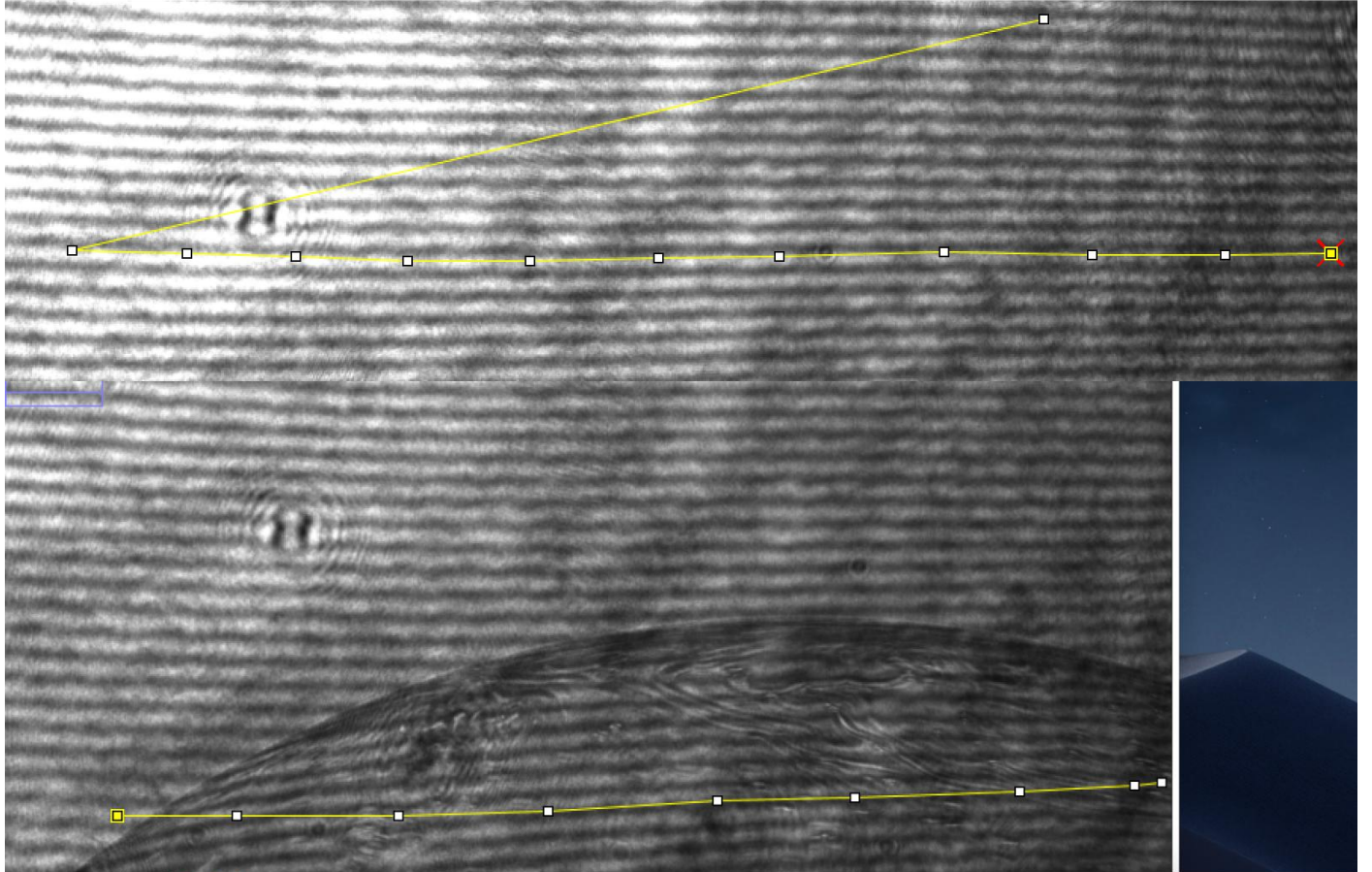
Below can be found the data processed using ImageJ, on my lab partner's Macbook.

In all, we did the popping of 9 bubbles, each at different concentrations of bubble mixture (3 each beginning with normal, less concentrated, more concentrated), to confirm our prediction that this would have no effect. We had slight clippings of the laser, but our interference patterns seemed unaffected by this.

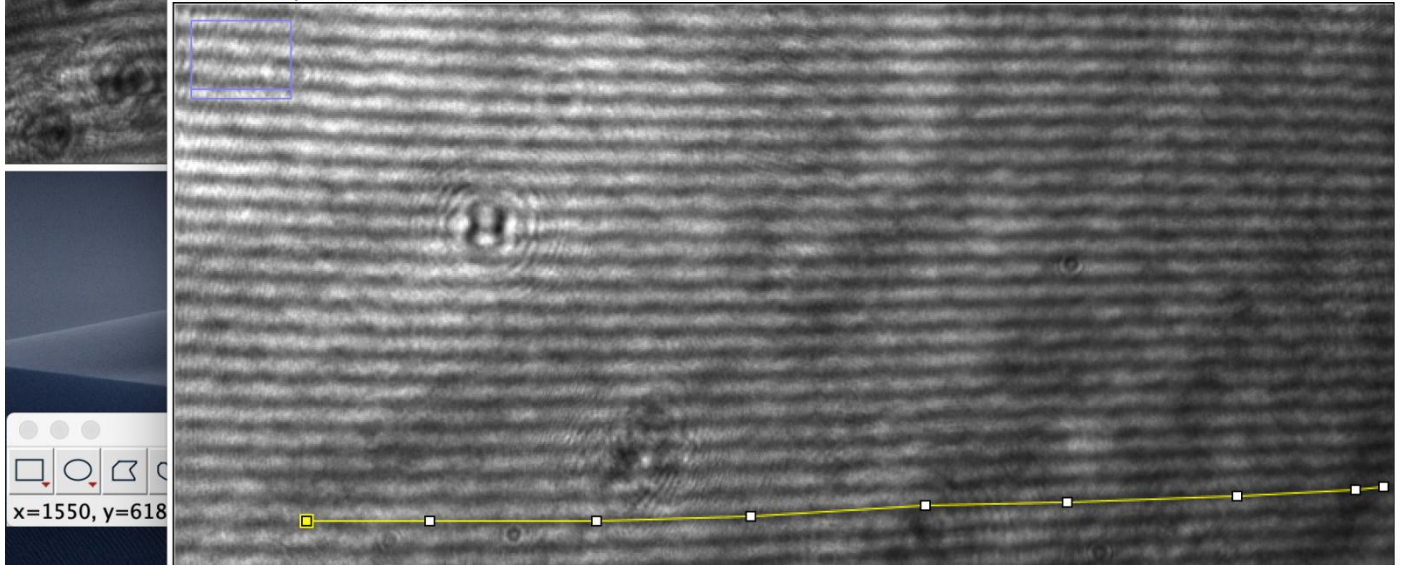


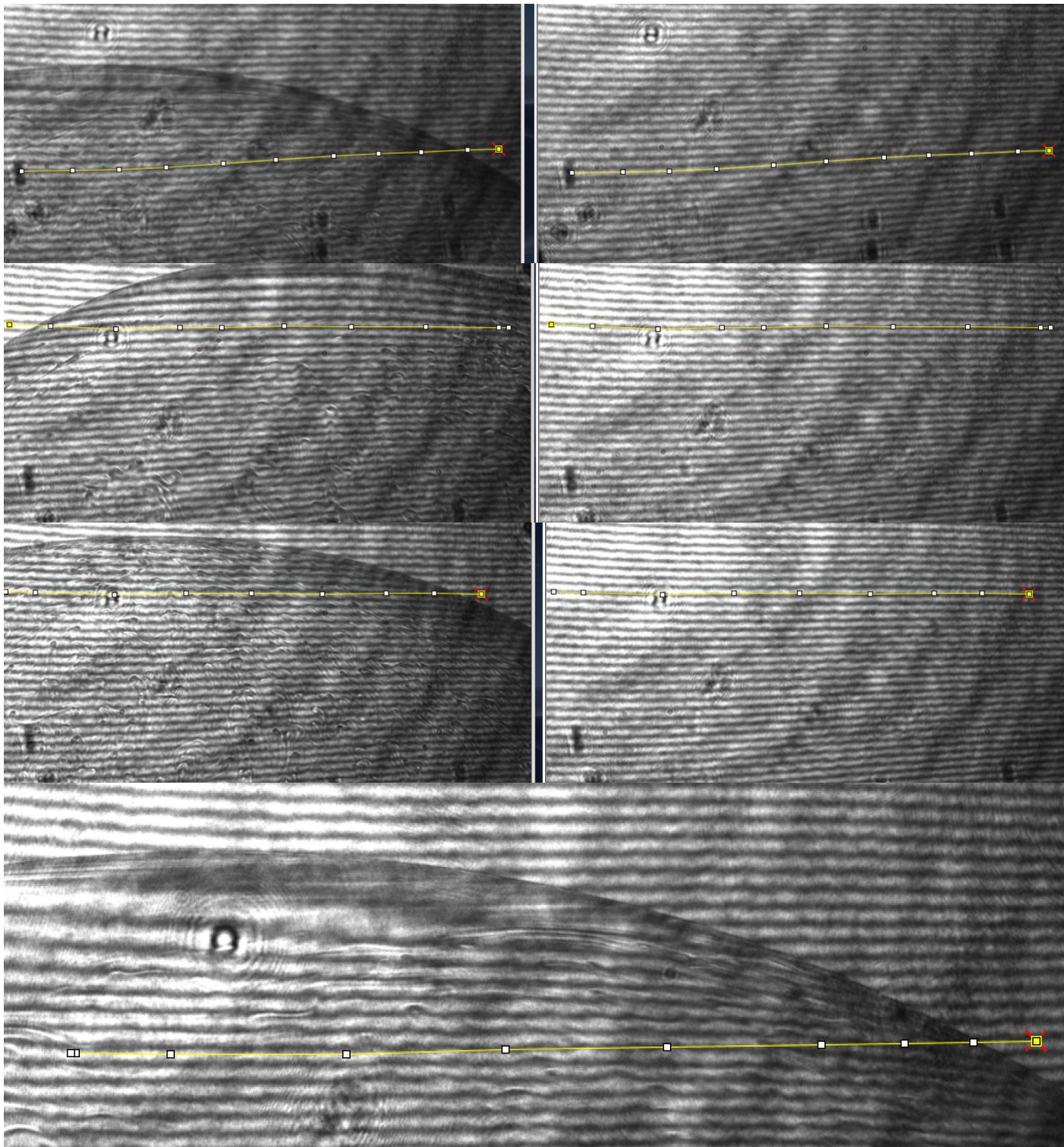


Screenshot 2021-12-05 at 02.53.08.png (50%)
x1234 pixels; RGB; 8.8MB

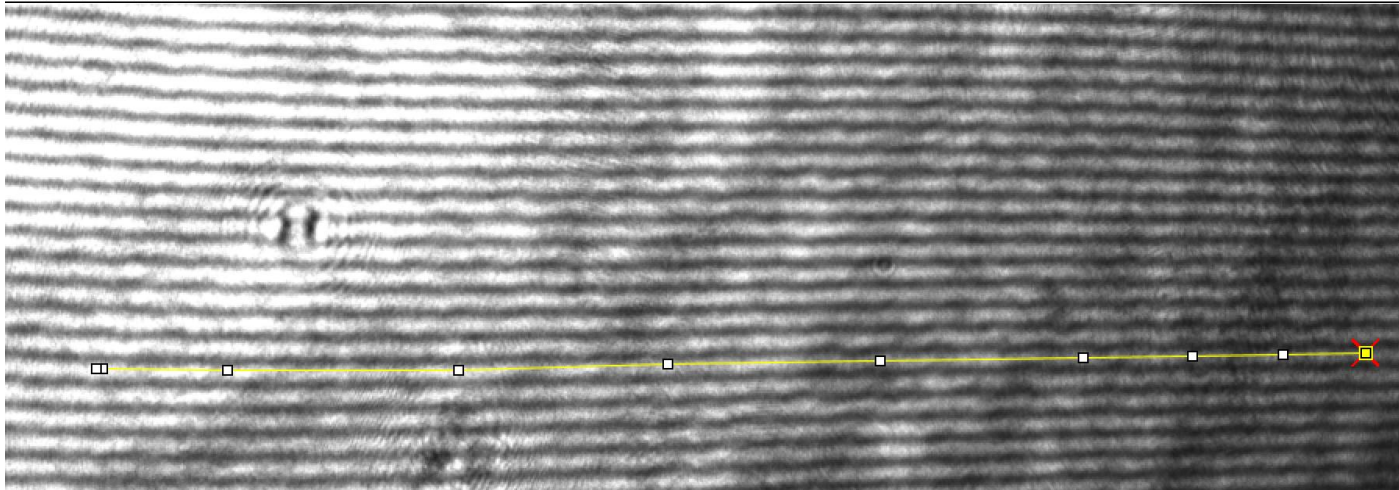


Screenshot 2021-12-05 at 02.44.32.png (50%)
1564x1234 pixels; RGB; 7.4MB

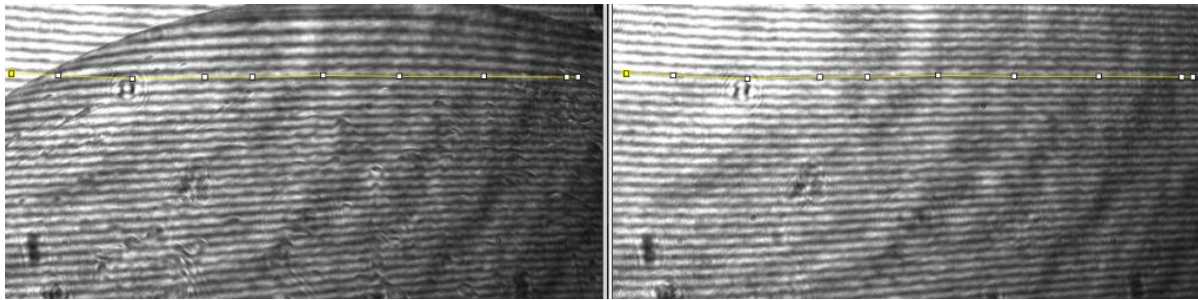




376x1234 pixels; RGB; 8.8MB Screenshot 2021-12-05 at 03.00.45.png (50%)



Through the comparison of the two images, such as the one shown below, we can ascertain F to be calculated through simply counting the number of fringes in the image, without the film intercepts, and subsequently we arrive at a value for the thickness of this film.



Data Analysis

As a result, the following table was obtained, which displays the Fringe Shift, and subsequent film thickness.

Bubble Number	Fringe Shift	Thickness of Film / m
1	2	3.33E-06
2	2	3.33E-06
3	3	5.00E-06
4	2	3.33E-06
5	3	5.00E-06
6	3	5.00E-06
7	3	5.00E-06
8	1	1.67E-06
9	3	5.00E-06

Sources of Uncertainty

λ (Wavelength of light in the laser) / nm	550 \pm 30nm As the light originating from the laser was green, and the following is the range of wavelengths green light takes on.
Thickness of Film / m	$\pm 1.67 \times 10^{-6}$ m Values for fringe shift vary from $F = 1$ to $F = 3$, therefore there is an absolute error equivalent to $F=1$, which corresponds to a thickness as shown.
Total Uncertainty	$\pm 1.67 \times 10^{-6}$ m

Summary

Therefore, in summary, we obtained the mean thickness of the average soap bubble, across all 9 soap bubbles, to have a value of $(4.07 \pm 1.67) \mu\text{m}$. The values for each individual bubble can be found above. However, when compared with reference values obtained from other online sources, we found our soap bubble thickness to be much thicker than the ranges given, having used refractive indexes of $N_{\text{air}} = 1$ and $N_{\text{soap}} = 1.33$.

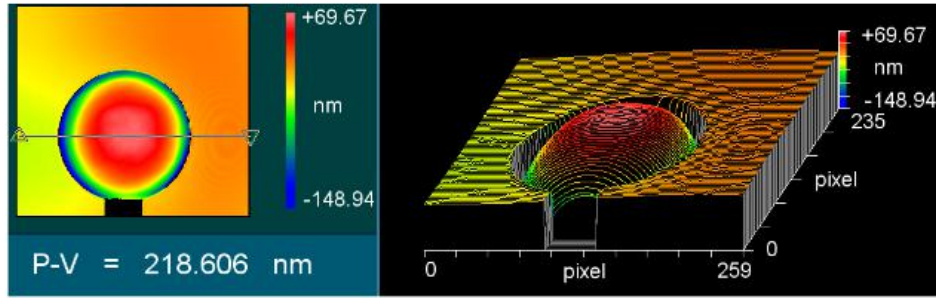


Fig. 6. Single-pass *OPD* map obtained with standard phase-shift acquisition and processing.

Although only within some approximation, the consistency of the measurement with the approach detailed in Section 4 is confirmed by a simple estimate of the bubble thickness from the *OPD* map given in Fig. 6. The *OPD* profile selected with a line through the central part of such a map is shown in Fig. 7. Using inspectors provided by the software of the interferometer, it is seen that the bubble occupies a lateral distance of 144 pixels. Taking such a distance as the bubble diameter, a reduction by a factor 0.8 leads to 115 pixels. Still working with inspectors, it is seen that the peak-to-valley of the central part of the profile for a width of 115 pixels is 88 nm. In Fig. 2 it is shown that the *OPD* difference between $q = 0.0$ and $q = 0.8$ for $d = 100$ nm is approximately 27 nm. The thickness estimate of our soap bubble is then $(88/27) \cdot 100$ nm = 326 nm. Although it is obtained using a single profile of the bubble instead of the entire bubble cap within $q = 0.8$, and also with some rough approximations, such a value is compatible with the result of 313 ± 14 nm computed with the general procedure described in Section 4.

Figure 3: The value of thickness of the soap bubble, as estimated in a research paper

Source: <https://www.osapublishing.org/viewmedia.cfm?seq=0&uri=oe-21-17-19657>, Vannoni et. al, 25th April 2013, "Measuring the thickness of soap bubbles with phase-shift interferometry "

For instance, the following source in Figure 3 found the soap bubble to have a thickness of roughly $0.33\mu\text{m}$. Consequently, our data exhibited a likely exhibited a large systematic shift, in an essence since the CMOD camera had been measuring the thickness of something other than simply the soap bubble.